1

INORGANIC CHEMISTRY ESSENTIALS

1.1 INTRODUCTION

Bioinorganic chemistry involves the study of metal species in biological systems. As an introduction to the basic inorganic chemistry needed for understanding bioinorganic topics, this chapter will discuss the essential chemical elements, the occurrences and purposes of metal centers in biological species, the geometries of ligand fields surrounding these metal centers, and ionic states preferred by the metals. Important considerations include equilibria between metal centers and their ligands and a basic understanding of the kinetics of biological metal–ligand systems. The occurrence of organometallic complexes and clusters in metalloproteins will be discussed briefly, and an introduction to electron transfer in coordination complexes will be presented. Since the metal centers under consideration are found in a biochemical milieu, basic biochemical concepts, including a discussion of proteins and nucleic acids, are presented in Chapter 2.

1.2 ESSENTIAL CHEMICAL ELEMENTS

Chemical elements essential to life forms can be broken down into four major categories: (1) bulk elements (H/H^+, C, N, $O^{2-}/O_2^{\cdot-}/O_2^{2-}$, P, S/S^{2-}); (2) macrominerals and ions (Na/Na^+, K/K^+, Mg/Mg^{2+}, Ca/Ca^{2+}, Cl^-, PO_4^{3-}, SO_4^{2-}); (3) trace

Bioinorganic Chemistry: A Short Course, Second Edition, by Rosette M. Roat-Malone

elements (Fe/Fe^{II}/Fe^{III}/Fe^{IV}, Zn/Zn^{II}, Cu/Cu^{I}/$Cu^{II}Cu^{III}$); and (4) ultratrace elements, comprised of nonmetals (F/F^-, I/I^-, Se/Se^{2-}, Si/Si^{IV}, As, B) and metals (Mn/Mn^{II}/Mn^{III}/Mn^{IV}, Mo/Mo^{IV}/Mo^{V}/Mo^{VI}, Co/Co^{II}/Co^{III}, Cr/Cr^{III}/Cr^{VI}, V/V^{III}/V^{IV}/V^{V}, Ni^{I}/Ni^{II}/Ni^{III}, Cd/Cd^{2+}, Sn/Sn^{II}/Sn^{IV}, Pb/Pb^{2+}, Li/Li^+). In the preceding classification, only the common biologically active ion oxidation states are indicated. (See references 3 and 21d for more information.) If no charge is shown, the element predominately bonds covalently with its partners in biological compounds, although elements such as carbon (C), sulfur (S), phosphorus (P), arsenic (As), boron (B), selenium (Se) have positive formal oxidation states in ions containing oxygen atoms; that is, S = +6 in the SO_4^{2-} ion or P = +5 in the PO_4^{3-} ion. The identities of essential elements are based on historical work and that done by Klaus Schwarz in the 1970s.[1] Other essential elements may be present in various biological species. Essentiality has been defined by certain criteria: (1) A physiological deficiency appears when the element is removed from the diet; (2) the deficiency is relieved by the addition of that element to the diet; and (3) a specific biological function is associated with the element.[2] Table 1.1 indicates the approximate percentages by weight of selected essential elements for an adult human.

Every essential element follows a dose–response curve, shown in Figure 1.1, as adapted from reference 2. At lowest dosages the organism does not survive, whereas in deficiency regions the organism exists with less than optimal function. After the concentration plateau of the optimal dosage region, higher dosages cause toxic effects in the organism, eventually leading to lethality. Specific daily requirements of essential elements may range from microgram to gram quantities as shown for two representative elements in Figure 1.1.[2]

Considering the content of earth's contemporary waters and atmospheres, many questions arise as to the choice of essential elements at the time of life's origins 3.5 billion or more years ago. Certainly, sufficient quantities of the bulk elements were available in primordial oceans and at shorelines. However, the concentrations of essential trace metals in modern oceans may differ considerably from those found in prebiotic times. Iron's current approximate 10^{-4} mM

TABLE 1.1 Percentage Composition of Selected Elements in the Human Body

Element	Percentage (by weight)	Element	Percentage (by weight)
Oxygen	53.6	Silicon, magnesium	0.04
Carbon	16.0	Iron, fluorine	0.005
Hydrogen	13.4	Zinc	0.003
Nitrogen	2.4	Copper, bromine	$2. \times 10^{-4}$
Sodium, potassium, sulfur	0.10	Selenium, manganese, arsenic, nickel	$2. \times 10^{-5}$
Chlorine	0.09	Lead, cobalt	$9. \times 10^{-6}$

Source: Adapted from reference 2.

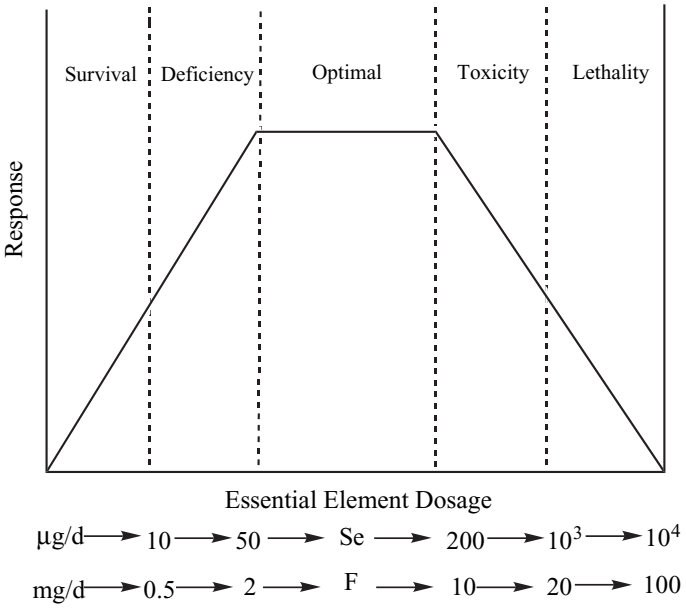

Figure 1.1 Dose–response curve for an essential element. (Used with permission from reference 2. Copyright 1985, Division of Chemical Education, Inc.)

concentration in seawater, for instance, may not reflect accurately its pre-life-forms availability. If one assumes a mostly reducing atmosphere contemporary with the beginnings of biological life, the availability of the more soluble iron(II) ion in primordial oceans must have been much higher. Thus, the essentiality of iron(II) at a concentration of 0.02 mM in the blood plasma heme (hemoglobin) and muscle tissue heme (myoglobin) may be explained. Besides the availability factor, many chemical and physical properties of elements and their ions are responsible for their inclusion in biological systems. These include: ionic charge, ionic radius, ligand preferences, preferred coordination geometries, spin pairings, systemic kinetic control, and the chemical reactivity of the ions in solution. These factors are discussed in detail by Frausto da Silva and Williams.[3]

1.3 METALS IN BIOLOGICAL SYSTEMS: A SURVEY

Metals in biological systems function in a number of different ways. Group 1 and 2 metals operate as structural elements or in the maintenance of charge and osmotic balance (Table 1.2). Transition metal ions that exist in single oxidation states, such as zinc(II), function as structural elements in superoxide dismutase and zinc fingers, or, as an example from main group +2 ions, as triggers for protein activity—that is, calcium ions in calmodulin or troponin C

TABLE 1.2 Metals in Biological Systems: Charge Carriers

Metal	Coordination Number, Geometry	Preferred Ligands	Functions and Examples
Sodium, Na^+	6, octahedral	*O*-Ether, hydroxyl, carboxylate	Charge carrier, osmotic balance, nerve impulses
Potassium, K^+	6–8, flexible	*O*-Ether, hydroxyl, carboxylate	Charge carrier, osmotic balance, nerve impulses

TABLE 1.3 Metals in Biological Systems: Structural, Triggers

Metal	Coordination Number, Geometry	Preferred Ligands	Functions and Examples
Magnesium, Mg^{2+}	6, octahedral	*O*-Carboxylate, phosphate	Structure in hydrolases, isomerases, phosphate transfer, trigger reactions
Calcium, Ca^{2+}	6–8, flexible	*O*-Carboxylate, carbonyl, phosphate	Structure, charge carrier, phosphate transfer, trigger reactions
Zinc, Zn^{2+} (d^{10})	4, tetrahedral	*O*-Carboxylate, carbonyl, *S*-thiolate *N*-imidazole	Structure in zinc fingers, gene regulation, anhydrases, dehydrogenases
Zinc, Zn^{2+} (d^{10})	5, square pyramid	*O*-Carboxylate, carbonyl, *N*-imidazole	Structure in hydrolases, peptidases
Manganese, Mn^{2+} (d^5)	6, octahedral	*O*-Carboxylate, phosphate, *N*-imidazole	Structure in oxidases, photosynthesis
Manganese, Mn^{3+} (d^4)	6, tetragonal	*O*-Carboxylate, phosphate, hydroxide	Structure in oxidases, photosynthesis

(Table 1.3). Transition metals that exist in multiple oxidation states serve as electron carriers—that is, iron ions in cytochromes or in the iron–sulfur clusters of the enzyme nitrogenase or copper ions in cytochrome c oxidase (Cu_A site), azurin and plastocyanin (Table 1.4); as facilitators of oxygen transport—that is, iron ions in hemoglobin or copper ions in hemocyanin (Table 1.5); and as sites at which enzyme catalysis occurs—that is, copper ions in superoxide dismutase or cytochrome c oxidase (Cu_B site), iron ions in heme a_3 of cytochrome c oxidase, or iron and molybdenum ions in nitrogenase (Table 1.6). Metal ions may serve multiple functions, depending on their oxidation state or location within the biological system so that the classifications in Tables 1.2–1.6 are necessarily incomplete, arbitrary, and/or overlapping.[4,5]

TABLE 1.4 Metals in Biological Systems: Electron Transfer

Metal	Coordination Number, Geometry	Preferred Ligands	Functions and Examples
Iron, Fe^{2+} (d^6)	4, tetrahedral	*S*-Thiolate	Electron transfer, nitrogen fixation in nitrogenases
Iron, Fe^{2+} (d^6)	6, octahedral	*O*-Carboxylate, alkoxide, oxide, phenolate	Electron transfer in oxidases
Iron, Fe^{3+} (d^5)	4, tetrahedral	*S*-Thiolate	Electron transfer, nitrogen fixation in nitrogenases
Iron, Fe^{3+} (d^5)	6, octahedral	*O*-Carboxylate, alkoxide, oxide, phenolate	Electron transfer in oxidases
Copper, Cu^{+} (d^{10}), Cu^{2+} (d^9)	3, trigonal planar	*N*-Imidazole	Electron transfer in Type III heme–copper oxidases (Cu_B in cytochrome c oxidase, for example)
Copper, Cu^{+} (d^{10}), Cu^{2+} (d^9)	4, tetrahedral	*S*-Thiolate, thioether, *N*-imidazole	Electron transfer in Type I blue copper proteins and Type III heme–copper oxidases (Cu_A in cytochrome c oxidase, for example)

TABLE 1.5 Metals in Biological Systems: Dioxygen Transport

Metal	Coordination Number, Geometry	Preferred Ligands	Functions and Examples
Copper, Cu^{2+} (d^9)	5, square pyramid 6, tetragonal	*O*-Carboxylate, *N*-imidazole	Type II copper oxidases, hydoxylases Type III copper hydroxylases, dioxygen transport in hemocyanin
Iron, Fe^{2+} (d^6)	6, octahedral	*N*-Imidazole, porphyrin	Dioxygen transport in hemoglobin and myoglobin

TABLE 1.6 Metals in Biological Systems: Enzyme Catalysis

Metal	Coordination Number, Geometry	Preferred Ligands	Functions and Examples
Copper, Cu^{2+} (d^9)	4, square planar	*O*-Carboxylate, *N*-imidazole	Type II copper in oxidases
Cobalt, Co^{2+} (d^7)	4, tetrahedral	*S*-Thiolate, thioether, *N*-imidazole	Alkyl group transfer, oxidases
Cobalt, Co^{3+} (d^6)	6, octahedral	*O*-Carboxylate, *N*-imidazole	Alkyl group transfer in vitamin B_{12} (cyanocobalamin)
Cobalt, Co^{2+} (d^7)	6, octahedral	*O*-Carboxylate *N*-imidazole	Alkyl group transfer in vitamin B_{12r}
Cobalt, Co^{+} (d^8)	6, octahedral, usually missing the 6th ligand	*O*-Carboxylate, *N*-imidazole	Alkyl group transfer in vitamin B_{12s}
Nickel, Ni^{2+} (d^8)	4, square planar	*S*-Thiolate, thioether, *N*-imidazole, polypyrrole	Hydrogenases, hydrolases
Nickel, Ni^{2+} (d^8)	6, octahedral		Uncommon
Molybdenum, Mo^{4+} (d^2), Mo^{5+} (d^1), Mo^{6+} (d^0)	6, octahedral	*O*-Oxide, carboxylate, phenolate, *S*-sulfide, thiolate	Nitrogen fixation in nitrogenases, oxo transfer in oxidases

1.4 INORGANIC CHEMISTRY BASICS

Ligand preference and possible coordination geometries of the metal center are important bioinorganic principles. Metal ligand preference is closely related to the hard–soft acid–base nature of metals and their preferred ligands. These are listed in Table 1.7.[6]

In general, hard metal cations form their most stable compounds with hard ligands, whereas soft metal cations form their most stable compounds with soft ligands. Hard cations can be thought of as small dense cores of positive charge, whereas hard ligands are usually the small highly electronegative elements or ligand atoms within a hard polyatomic ion—that is, oxygen ligands in $(RO)_2PO_2^-$, or $CH_3CO_2^-$. Crown ethers are hard ligands that have cavities suitable for encapsulating hard metal ions. The [18]-crown-6 ether shown in Figure 1.2 with its 2.6 to 3.2-Å hole provides a good fit for the potassium ion, which has a radius of 2.88 Å.[6]

It is possible to modify a hard nitrogen ligand toward an intermediate softness by increasing the polarizability of its substituents or the π electron cloud

TABLE 1.7 Hard–Soft Acid–Base Classification of Metal Ions and Ligands

Metals, Ions, Molecules				Ligands
HARD				HARD
H^+	Mg^{2+}	Al^{3+}	SO_3	Oxygen ligands in H_2O, CO_3^{2-}, NO_3^-, PO_4^{3-},
Na^+	Ca^{2+}	Co^{3+}	CO_2	$ROPO_3^{2-}$, $(RO)_2PO_2^-$, CH_3COO^-, OH^-, RO^-,
K^+	Mn^{2+}	Cr^{3+}		R_2O, and crown ethers
	VO^{2+}	Ga^{3+}		Nitrogen ligands in NH_3, N_2H_4, RNH_2, or Cl^-
		Fe^{3+}		
		Tl^{3+}		
		Ln^{3+}		
		MoO^{3+}		
INTERMEDIATE				INTERMEDIATE
Fe^{2+}, Ni^{2+}, Zn^{2+}, Co^{2+}, Cu^{2+}, Pb^{2+}, Sn^{2+}, Ru^{2+}, Au^{3+}, SO_2, NO^+				Br^-, SO_3^{2-}, Nitrogen ligands in NO_2^-, N_3^-, N_2, 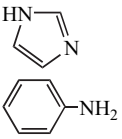
SOFT				SOFT
Cu^+	Pt^{2+}	Pt^{4+}		Sulfur ligands in RSH, RS^-, R_2S, R_3P, RNC,
Au^+	Pb^{2+}			CN^-, CO, R^-, H^-, I^-, $S_2O_3^{2-}$, $(RS)_2PO_2^-$,
Tl^+	Hg^{2+}			$(RO)_2P(O)S^-$
Ag^+	Cd^{2+}			
Hg_2^{2+}	Pd^{2+}			

Source: Adapted from references 4 and 6.

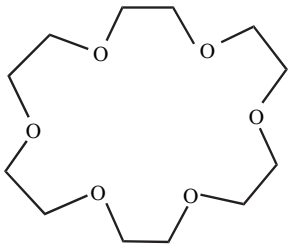

Figure 1.2 [18]-Crown-6 ether.

about it, an example being the imidazole nitrogen of the amino acid histidine. Increasing the softness of phosphate ion substituents can transform the hard oxygen ligand of $(RO)_2PO_2^-$ to a soft state in $(RS)_2PO_2^-$. Soft cations and anions are those with highly polarizable, large electron clouds—that is, Hg^{2+}, sulfur ligands as sulfides or thiolates, and iodide ions. Also, note that metal ions can overlap into different categories. Lead as Pb^{2+}, for instance, appears in both the intermediate and soft categories. The Fe^{3+} ion, classified as a hard

cation, coordinates to histidine (imidazole) ligands in biological systems, whereas Fe^{2+}, classified as intermediate, can coordinate to sulfur ligands and the carbon atom of CO (see Section 7.2, for example, in which hemoglobin and myoglobin are discussed).

1.5 BIOLOGICAL METAL ION COMPLEXATION

1.5.1 Thermodynamics

The thermodynamic stability of metal ions is denoted by stepwise formation constants as shown in equations 1.1–1.3 (charges omitted for simplicity):

$$\mathrm{M + L \leftrightarrow ML} \qquad K_1 = \frac{[\mathrm{ML}]}{[\mathrm{M}][\mathrm{L}]} \tag{1.1}$$

$$\mathrm{ML + L \leftrightarrow ML_2} \qquad K_2 = \frac{[\mathrm{ML_2}]}{[\mathrm{M}][\mathrm{L}]} \tag{1.2}$$

$$\mathrm{ML_2 + L \leftrightarrow ML_3} \qquad K_3 = \frac{[\mathrm{ML_3}]}{[\mathrm{ML_2}][\mathrm{L}]} \tag{1.3}$$

Alternately, they are indicated by overall stability constants as shown in equations 1.4–1.6:

$$\mathrm{M + L \leftrightarrow ML} \qquad \beta_1 = \frac{[\mathrm{ML}]}{[\mathrm{M}][\mathrm{L}]} \tag{1.4}$$

$$\mathrm{M + 2L \leftrightarrow ML_2} \qquad \beta_2 = \frac{[\mathrm{ML}]}{[\mathrm{M}][\mathrm{L}]^2} \tag{1.5}$$

$$\mathrm{M + 3L \leftrightarrow ML_3} \qquad \beta_3 = \frac{[\mathrm{ML}]}{[\mathrm{M}][\mathrm{L}]^3} \tag{1.6}$$

The equation relating the stepwise and overall stability constants is indicated by equation 1.7:

$$\beta_n = K_1 K_2 \ldots \mathrm{K}_n \tag{1.7}$$

In biological systems, many factors affect metal–ligand complex formation. Hard–soft acid–base considerations have already been mentioned. Concentrations of the metal and ligand at the site of complexation are determined locally through concentration gradients, membrane permeability to metals and ligands, and other factors. Various competing equilibria—solubility products, complexation, and/or acid–base equilibrium constants—sometimes referred to as "metal ion speciation," all affect complex formation. Ion size and charge, preferred metal coordination geometry, and ligand chelation effects all affect metal uptake. To better measure biological metal–ligand interactions, an

TABLE 1.8 K_{ML} and $K_{ML} \times [M]$ for Some Cations and Their Differentiating Ligands

	K^+, Na^+	Ca^{2+}, Mg^{2+}	Zn^{2+}, Cu^{2+}	Differentiating Ligand
K^+, Na^+				*O*-Macrocycles such as crown ethers, cryptates and naturally occurring macrocyclic antibiotics such as nonactin and valinomycin
K_{ML}	>10	$<10^2$	$<10^6$	
$K_{ML} \times [M]$	>1.0	<0.1	<0.1	
Ca^{2+}, Mg^{2+}				Oxygen donors such as di- or tricarboxylates
K_{ML}	1.0	$<10^3$	$<10^6$	
$K_{ML} \times [M]$	<0.1	>1.0	<0.1	
Zn^{2+}, Cu^{2+}				Nitrogen and sulfur ligands
K_{ML}	0.1	$<10^2$	$>10^6$	
$K_{ML} \times [M]$	<0.1	<0.1	>1.0	

Source: Adapted from reference 3.

"uptake factor" is defined as $K_{ML} \times [M]$, where K_{ML} is the stability constant K_1 and [M] is the concentration of metal ion. Since naturally occurring aqueous systems have metal ion concentration varying roughly as

K^+, Na^+	Ca^{2+}, Mg^{2+}	Zn^{2+}	Cu^{2+}	Fe^{2+}
10^{-1} M	~10^{-3} M	<10^{-9} M	<10^{-12} M	~10^{-17} M

great selectivity for metal species is necessary to concentrate the necessary ions at sites where they are needed. Differentiating ligands are those preferred by the cation in question. A much more detailed discussion takes place in reference 3. Table 1.8 is adapted from this source.

1.5.2 Kinetics

As students learned in their introductory chemistry courses, rates of reaction are divided into several classes, depending on the number of reactants involved in rate determination. These are: (1) zero order—the reaction rate is independent of the concentration of that reactant; (2) first order—the reaction rate is dependent on the concentration of one reactant; (3) second order—the reaction rate is dependent on the concentration of two reactants; and (4) higher order—the reaction rate is dependent on more than two reactants. Higher-order reaction rates are very rare because the possibility of bringing more than two reactants together productively is very small. Bioinorganic kineticists, studying the reaction rates of complex enzymatic reactions, often simplify matters to isolate a reaction of interest and relate it to a proposed mechanism for the enzyme's catalytic activity. For instance, in a pseudo-zero-order reaction—that is, one that would be first order under normal circumstances—the concentration of the enzyme may be held constant while a particular substrate's concentration is varied but does not affect the reaction rate. This condition may apply when the enzyme is saturated with substrate over the range of

substrate concentration studied. In a pseudo-first-order reaction—that is, one that would normally be second order—the concentration of one reactant is held constant while the other is varied so that the reaction rate is directly proportional to the reactant whose concentration is varied. This is the most commonly used experimental technique used by enzyme kineticists.

In biological systems, as in all others, metal ions exist in an inner coordination sphere, an ordered array of ligands binding directly to the metal. Surrounding this is the outer coordination sphere consisting of other ligands, counterions, and solvent molecules. In stoichiometric mechanisms where one can distinguish an intermediate, substitution within the metals inner coordination sphere may take place through an associative (A), S_N2 process as shown in equations 1.8 (for six-coordinate complexes) and 1.9 (for four-coordinate complexes) or a dissociative (D), S_N1 mechanism as shown in equation 1.10 (RDS = rate determining step).

$$ML_6^{n+} + L' \xrightarrow{\text{RDS}} ML_6L'^{n+} \rightarrow ML_5L'^{n+} + L \tag{1.8}$$

$$ML_4^{n+} + L' \xrightarrow{\text{RDS}} ML_4L'^{n+} \rightarrow ML_3L'^{n+} + L \tag{1.9}$$

$$ML_6^{n+} \xrightarrow{\text{RDS}} ML_5L^{n+} + L' \xrightarrow{\text{fast}} ML_5L'^{n+} + L \tag{1.10}$$

Associative mechanisms for metals in octahedral fields are difficult stereochemically (due to ligand crowding); therefore, they are rare for all but the largest metal ion centers. The associative mechanism is well known and preferred for four-coordinate square-planar complexes. Pure dissociative mechanisms are rare as well. When an intermediate cannot be detected by kinetic, stereochemical, or product distribution studies, the so-called interchange mechanisms (I) are invoked. Associative interchange (I_A) mechanisms have rates dependent on the nature of the entering group, whereas dissociative interchange (I_D) mechanisms do not.

The simplest reactions to study, those of coordination complexes with solvent, are used to classify metal ions as labile or inert. Factors affecting metal ion lability include size, charge, electron configuration, and coordination number. Solvents can by classified as to their size, polarity, and the nature of the donor atom. Using the water exchange reaction for the aqua ion $[M(H_2O)_n]^{m+}$, metal ions are divided by Cotton, Wilkinson, and Gaus[7] into four classes:

Class I. Rate constants for water exchange exceed $10^8\,s^{-1}$, essentially diffusion controlled. These are classified as the labile species.

Class II. Rate constants for water exchange are in the range 10^4–$10^8\,s^{-1}$.

Class III. Rate constants for water exchange are in the range 1–$10^4\,s^{-1}$.

Class IV. Rate constants for water exchange are in the range 10^{-3}–$10^{-6}\,s^{-1}$. These ions are classified as inert.

Labile species are usually main group metal ions with the exception of Cr^{2+} (high-spin $3d^4$) and Cu^{2+} ($3d^9$) whose lability can be ascribed to Jahn–Teller

TABLE 1.9 Rate Constants for Water Exchange in Metal Aqua Ions

Class	Metal Ions	Rates $\log k$ (s^{-1})
I	Group IA (1), Group IIA (2) except Be and Mg, Group IIB (12) except Zn^{2+} ($3d^{10}$), Cr^{2+} ($3d^4$), Cu^{2+} ($3d^9$)	8–9
II	Zn^{2+} ($3d^{10}$)	7.6
	Mn^{2+} ($3d^5$)	6.8
	Fe^{2+} ($3d^6$)	6.3
	Co^{2+} ($3d^7$)	5.7
	Ni^{2+} ($3d^8$)	4.3
	Mg^{2+}	6.0
III	Ga^{3+}	3.0
	Be^{2+}	2.0
	V^{2+} ($3d^3$)	2.0
	Al^{3+}	<0.1
IV	Cr^{3+} ($3d^3$), Co^{3+} ($3d^6$), Rh^{3+} ($3d^6$), Ir^{3+} ($3d^6$), Pt^{2+} ($3d^8$)	–3 to –6

Source: Adapted from references 7 and 8.

effects. Section 1.6 includes a formula for determining the number of *d* electrons in a transition metal ion, and Figures 1.4 and 1.7 show the placement of *d* electrons into nondegenerate (split) *d* orbitals in various ligand fields. Jahn–Teller effects arise (for the high-spin $3d^4$ case) because the lone electron in the two destabilized, but degenerate, e_g orbitals causes further splitting of the e_g level with consequences for bond lengths between the metal ion and its ligands. Filling in the octahedral energy level diagram for the Cu^{2+} ($3d^9$) case in Figure 1.4, readers should be able to show three electrons in the e_g level, again causing a loss of degeneracy in these orbitals. Transition metals of classes II and III are species with small ligand field stabilization energies, whereas the inert species have high ligand field stabilization energies (LFSE). Examples include Cr^{3+} ($3d^3$) and Co^{3+} ($3d^6$). Jahn–Teller effects and LFSE are further discussed in Section 1.6. Table 1.9 reports rate constant values for some aqueous solvent exchange reactions.[8]

Outer-sphere (OS) reaction rates and rate laws can be defined for solvolysis of a given complex. Complex formation is defined as the reverse reaction—that is, replacement of solvent (S) by another ligand (L′). Following the arguments of Tobe,[9] in aqueous solution the general rate law for complex formation (eliminating charge for simplicity),

$$[\mathrm{M(L}_n\mathrm{)(S)}] + \mathrm{L}' \rightarrow [\mathrm{M(L}_n\mathrm{)(L}')] + \mathrm{S} \tag{1.11}$$

takes the second-order form shown in equation 1.12:

$$-d\frac{[\mathrm{M(L}_n\mathrm{)(S)}]}{dt} = k'[\mathrm{M(L}_n\mathrm{)(S)}][\mathrm{L}'] \tag{1.12}$$

The rate law frequently may be more complex and given as equation 1.13:

$$-d\frac{[\mathrm{M(L}_n\mathrm{)(S)}]}{dt} = \frac{k'\mathrm{K}[\mathrm{M(L}_n\mathrm{)(S)}][\mathrm{L}']}{(1+\mathrm{K}[\mathrm{L}'])} \tag{1.13}$$

Equation 1.13 reduces to the second-order rate law, shown in equation 1.12, when $K[\mathrm{L}'] <<< 1$ and to a first-order rate law, equation 1.14,

$$-d\frac{[\mathrm{M(L}_n\mathrm{)(S)}]}{dt} = k'[\mathrm{M(L}_n\mathrm{)(S)}] \tag{1.14}$$

when $K[\mathrm{L}'] >>> 1$.

Interchange mechanisms ($\mathrm{I_A}$ or $\mathrm{I_D}$) in a preformed outer sphere (OS) complex will generate the following observed rate laws (which cannot distinguish $\mathrm{I_A}$ from $\mathrm{I_D}$) with the equilibrium constant = K_{OS} (equation 1.15) and $k = k_{\mathrm{i}}$ (equation 1.16).

$$[\mathrm{M(L}_n\mathrm{)(S)}] + \mathrm{L}' \leftrightarrow [\mathrm{M(L}_n\mathrm{)(S)}]\ldots\mathrm{L}' \qquad K_{\mathrm{OS}} \tag{1.15}$$

$$[\mathrm{M(L}_n\mathrm{)(S)}]\ldots\mathrm{L}' \rightarrow [\mathrm{M(L}_n\mathrm{)(L}')]\ldots\mathrm{S} \qquad k_i \tag{1.16}$$

The dissociative (D or S_N1) mechanism, for which the intermediate is long-lived enough to be detected, will yield equations 1.18 and 1.19 where $k = k_1$ and $K = k_2/(k_{-1}[\mathrm{S}])$. For the reaction:

$$[\mathrm{M(L}_n\mathrm{)}] + \mathrm{S} \xrightarrow{k_1} [\mathrm{M(L}_n\mathrm{)(S)}], \text{ and its reverse,}$$

$$[\mathrm{M(L}_n\mathrm{)(S)}] \xrightarrow{k_{-1}} [\mathrm{M(L}_n\mathrm{)}] + \mathrm{S} \tag{1.17}$$

$$[\mathrm{M(L}_n\mathrm{)(S)}] \leftrightarrow [\mathrm{M(L}_n\mathrm{)}] + \mathrm{S} \qquad k_1k_{-1} \tag{1.18}$$

$$[\mathrm{M(L}_n\mathrm{)}] + \mathrm{L}' \rightarrow [\mathrm{M(L}_n\mathrm{)(L}')] \qquad k_2 \tag{1.19}$$

The associative (A or S_N2) will give the simple second-order rate law shown in equations 1.21 and 1.22 if the higher coordination number intermediate concentration remains small, resulting in the rate dependence shown in equation 1.23. For the reaction

$$[\mathrm{M(L}_n\mathrm{)(S)}] + \mathrm{L}' \xrightarrow{k_a} [\mathrm{M(L}_n\mathrm{)(S)(L}')], \text{ and its reverse,}$$

$$[\mathrm{M(L}_n\mathrm{)(S)(L}')] \xrightarrow{k_{-a}} [\mathrm{M(L}_n\mathrm{)(S)}] + \mathrm{L}' \tag{1.20}$$

we have

$$[\mathrm{M(L}_n\mathrm{)(S)}] + \mathrm{L}' \leftrightarrow [\mathrm{M(L}_n\mathrm{)(S)(L}')] \qquad k_ak_{-a} \tag{1.21}$$

$$[\mathrm{M(L}_n\mathrm{)(S)(L}')] \rightarrow [\mathrm{M(L}_n\mathrm{)(L}')] + \mathrm{S} \qquad k_b \tag{1.22}$$

$$-d\frac{[\mathrm{M(L}_n\mathrm{)(S)}]}{dt} = \frac{k_ak_b}{k_{-a}+k_b}[\mathrm{M(L}_n\mathrm{)(S)}][\mathrm{L}'] \tag{1.23}$$

In all cases the key to assigning mechanism is the ability to detect and measure the equilibrium constant K. The equilibrium constant K_{OS} can be estimated through the Fuoss–Eigen equation[10] as shown in equation 1.24. Usually, K_{OS} is ignored in the case of L′ = solvent.

$$K_{OS} = \frac{4\pi N_A a^3}{3000}(e^{-V/kT}) \tag{1.24}$$

where a is the distance of closest approach of the oppositely charged ions (~5 Å), N_A is Avogadro's number, and V is the electrostatic potential at that distance (equation 1.25).

$$V = \frac{Z_1 Z_2 e^2}{4\pi\varepsilon_0\varepsilon_R a} \tag{1.25}$$

where

a = distance of closest approach of oppositely charged ions (~5 Å)
N_A = Avogadro's number, $6.022 \times 10^{23}\,\text{mol}^{-1}$
V = electrostatic potential (dependent on distance between oppositely charged ions)
k = rate constant for a reaction
K = equilibrium constant for a reaction
Z_1Z_2 = absolute value of the charge on an ion
e = charge on the electron, 4.8030×10^{-10} esu or 1.6022×10^{-19} Coulombs (C)
$\varepsilon_0\varepsilon_R$: ε_0 = permittivity in a vacuum 8.854×10^{-12} (C^2/Jm), ε_R or ε_r = dielectric constant = relative permittivity = 1 (for vacuum by definition, 80.4 for H_2O at 20°C), $\varepsilon_0\varepsilon_R$ = actual permittivity

As the above discussion indicates, assigning mechanisms to simple anation reactions of transition metal complexes is not simple. The situation becomes even more difficult for a complex enzyme system containing a metal cofactor at an active site. Methods developed to study the kinetics of enzymatic reactions according to the Michaelis–Menten model will be discussed in Section 2.2.4. Since enzyme-catalyzed reactions are usually very fast, experimentalists have developed rapid kinetic techniques to study them. Techniques used by bioinorganic chemists to study reaction rates will be further detailed in Section 3.7.2.1 and 3.7.2.2.

1.6 ELECTRONIC AND GEOMETRIC STRUCTURES OF METALS IN BIOLOGICAL SYSTEMS

Tables 1.2–1.6 list some of the important geometries assumed by metal ions in biological systems. Common geometries adopted by transition metal ions that will be of most concern to readers of this text are illustrated in Figure 1.3. It is important to remember that in biological systems these geometries are usually distorted in both bond length and bond angle.

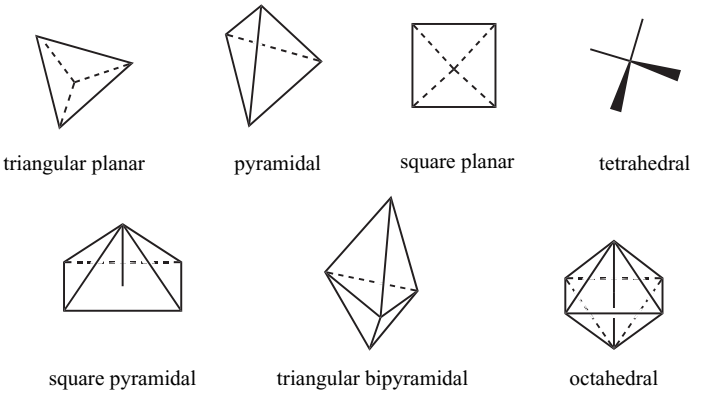

Figure 1.3 Common transition metal coordination geometries.

Transition metal ions play special roles in biological systems, with all elements from the first transition series except titanium (Ti) and scandium (Sc) occurring with great variety in thousands of diverse metalloproteins. Metal ions determine the geometry of enzymatic active sites, act as centers for enzyme reactivity, and act as biological oxidation–reduction facilitators. Molybdenum (Mo) appears to be the only transition element in the second transition series with a similar role. Vanadium (V), technetium (Tc), platinum (Pt), ruthenium (Ru), and gold (Au) compounds, as well as gadolinium (Gd) and other lanthanide complexes, are extremely important in medicinal chemistry. Tables 1.2–1.6 list the *d* electron configuration for transition metal ions common to biological systems. To find the number of *d* electrons for any transition metal ion, the following is a useful formula:

Number of *d* electrons = Atomic number for the element (Z) – oxidation state of the element's ion – Z for the preceding noble-gas element.

Examples: Fe(II): $26 - 2 - 18\,(\text{argon}) = 6$

Mo(V): $42 - 5 - 36\,(\text{krypton}) = 1$

Note that there are a number of different methods for indicating the oxidation state of a metal ion, especially transition metal ions that have variable oxidation states. As an example, the iron ion in its +2 oxidation state may be written as Fe^{2+}, Fe(II), Fe^{II}, or iron(II). In this text, the methods are used interchangeably.

As a consequence of their partially filled *d* orbitals, transition metals exhibit variable oxidation states and a rich variety of coordination geometries and ligand spheres. Although a free metal ion would exhibit degenerate *d* electron energy levels, ligand field theory describes the observed splitting of these *d* electrons for metal ions in various ligand environments. In all cases, the amount of stabilization or destabilization of *d* electron energy levels centers about the

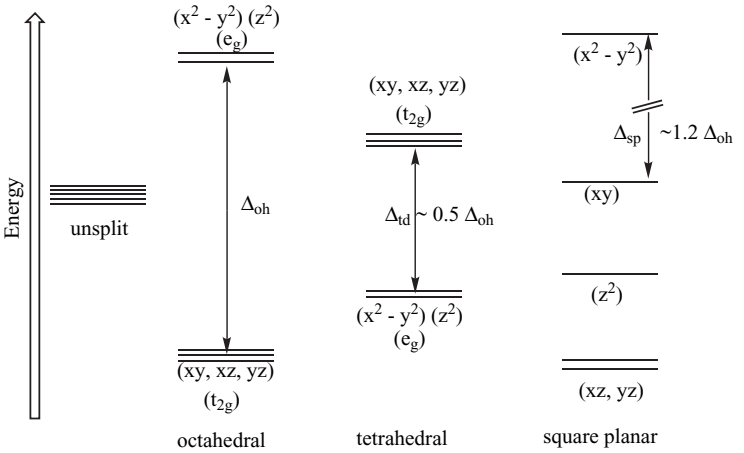

Figure 1.4 Approximate energy levels for *d* electrons in octahedral, tetrahedral, and square-planar fields.

so-called barycenter of unsplit *d* electron energy levels. The most important splittings for bioinorganic applications are shown in Figure 1.4 for octahedral, tetrahedral, and square-planar ligand fields. The t_{2g} (d_{xy}, d_{yz}, and d_{xz}) and e_g ($d_{x^2-y^2}$ and d_{z^2}) energy level designations identify symmetry properties of the *d* orbitals and are often used to indicate the degenerate energy levels under discussion. (See LFSE discussion below). Generally, the energy gap between stabilized and destabilized *d*-electron energy levels for tetrahedral fields (Δ_t) is approximately one-half that for octahedral fields (Δ_{oh}), and that for square-planar fields is approximately $1.2\Delta_{oh}$. Many thermodynamic and kinetic properties of transition metal coordination complexes can be predicted by knowing the magnitude of Δ. Measurement of ultraviolet and visible absorption spectra of transition metal complexes that arise from these quantum mechanically forbidden (but observed) *d–d* transitions provide a measure of Δ.

To describe the *d*-orbital splitting effect for the octahedral field, one should imagine ligand spheres of electron density approaching along the *x*, *y*, and *z* axes where the $d_{x^2-y^2}$ and d_{z^2} lobes of electron density point. Figure 1.5 illustrates representations of high-probability electron orbit surfaces for the five *d* orbitals.

For octahedral (O_h) geometry the repelling effect of like charge approach of the ligand electrons toward regions of high *d* electron density along the *x*, *y*, and *z* axes elevates the energy of the e_g ($d_{x^2-y^2}$ and d_{z^2}) orbitals while the t_2g (d_{xy}, d_{yz}, and d_{xz}) orbitals are proportionally lowered in energy. For the tetrahedral (T_d) case ligands approach between the *x*, *y*, and *z* axes, stabilizing $d_{x^2-y^2}$ and d_{z^2} and destabilizing d_{xy}, d_{yz}, and d_{xz} orbital energy levels. For the square-planar case, ligands will approach along the *x* and *y* axes. Distorted octahedral and tetrahedral geometries are quite common in biological systems. Octahedral geometries are found for iron ions in heme ligand systems to be discussed in Chapter 7—for instance, while copper ions occur in distorted

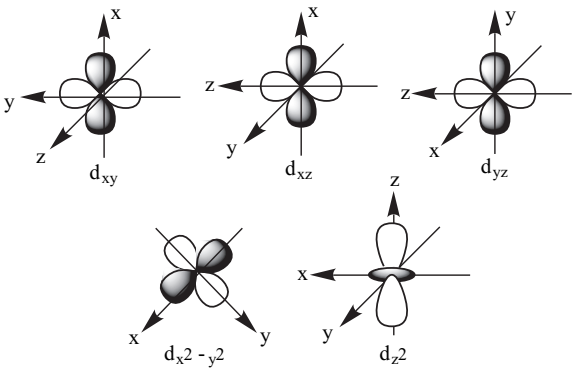

Figure 1.5 Representations of the five *d* orbitals along *x, y*, and *z* axes.

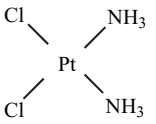

cis-dichlorodiammineplatinum(II)
cisplatin, cisDDP

Figure 1.6 The antitumor active platinum compound *cis*-dichlorodiammineplatinum (II).

pyramidal, tetrahedral, or even trigonal bipyramidal forms. Less commonly, square-planar geometries are found for d^8 transition metal ions, especially for gold(III), iridium(I), palladium(II), and platinum(II) and for nickel(II) species in strong ligand fields. The platinum anticancer agent, *cis*-dichlorodiammineplatinum(II), shown in Figure 1.6, has a square-planar geometry all important for its utilization as an antitumor agent. While the other geometries shown in Figure 1.3 might be less common for metal ions in biological species, they do occur (also with distorted bond distances and angles) and will be described in discussions of the metal center in the specific protein or enzyme.

The strength of the ligand field at a metal center is strongly dependent on the character of the ligand's electronic field and leads to the classification of ligands according to a "spectrochemical series" arranged below in order from weak field (halides, sulfides, hydroxides) to strong field (cyanide and carbon monoxide):

$$I^- < Br^- < S^{2-} < Cl^- < NO_3^- < OH^- \sim RCOO^- < H_2O \sim RS^- < NH_3 \sim \text{imidazole} < \text{en}$$
$$(\text{ethylenediamine or diaminoethane}) < \text{bpy}\ (2,2'\text{-bipyridine}) < CN^- < CO$$

Ligand field strength may determine coordination geometry. For example, $NiCl_4^{2-}$ occurs as a tetrahedral complex (small splitting—small Δ_{td}), whereas

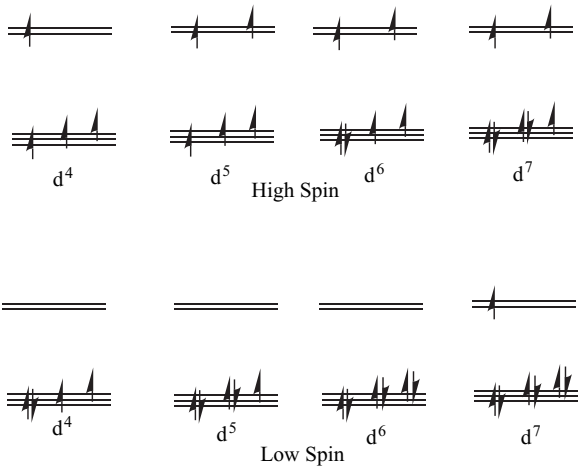

Figure 1.7 High-spin and low-spin *d*-electron configurations for the octahedral field.

$Ni(CN)_4^{2-}$ occurs in the square-planar geometry (large energy gap—large Δ_{sp}). In octahedral fields, ligand field strength can determine the magnetic properties of metal ions since for d^4 through d^7 electronic configurations both high-spin (maximum unpairing of electron spins) and low-spin (maximum pairing of electron spins) complexes are possible. Possible configurations are shown in Figure 1.7. In general, weak field ligands form high-spin (h.s.) complexes (small Δ_{oh}) and strong field ligands form low-spin (l.s.) complexes (large Δ_{oh}). Usually, tetrahedral complexes have high spin (small Δ_{td}) and will be paramagnetic. Square-planar complexes, usually found for metal ions having the electron configuration d^8, will be diamagnetic—all electrons paired—since a large energy gap occurs between the last filled orbital (d_{xy}) and the $d_{x^2-y^2}$ orbital (see Figure 1.4). Detection of paramagnetism (unpaired electrons) and diamagnetism (all electrons paired) in bioinorganic ligand fields can help determine coordination geometry at active enzymes sites. In the case of hemoglobin, for example, the d^6 iron(II) center cycles between high-spin (paramagnetic) and low-spin (diamagnetic) configurations. The change is evident in electron paramagnetic resonance (EPR) spectroscopy in which a spectrum is determined only for paramagnetic species. See Section 3.5. Placement of *d* electrons also affects the placement of the iron center in or out of the plane of its porphyrin ligand in hemoglobin or myoglobin—high-spin systems require more room so that a h.s. Fe(II) ion will move out of the porphyrin ligand's planar coordination sphere. See Section 7.2 for further discussion with respect to this phenomenon in myoglobin and hemoglobin. In Type III copper enzymes, two d^9 copper(II) centers become antiferromagnetically coupled resulting in a loss of the expected paramagnetism. See Section 7.8 for a discussion of binuclear copper centers in cytochrome c oxidase.

The sum of the *d* electron contributions to LFSE can be calculated with the formula shown in equation 1.26 for octahedral complexes.

$$\text{LFSE} = \frac{2}{5}(\#\, e^- \text{ in } t_{2g})\Delta_{\text{oh}} + \frac{3}{5}(\#\, e^- \text{ in } e_g)\Delta_{\text{oh}} \tag{1.26}$$

where $\#e^-$ is the number of *d* electrons.

The 2/5 stabilization (negative energy values) and 3/5 destabilization (positive energy values) modifiers arise from the displacement of three *d* orbitals to lower energy versus two *d* orbitals to higher energy from the unsplit degenerate *d* orbital state before imposition of the ligand field. Splitting values for *d* orbital energy levels, based on $\Delta_{\text{oh}} = 10$, has been adapted from reference 7 and appears in Table 1.10.

The Jahn–Teller effect arises in cases where removal of degeneracy of a *d*-electron energy level is caused by partial occupation of a degenerate level. Two common examples are those of Cu(II), d^9, and high spin Cr(II), d^4, as shown in Figure 1.8. Electrons in the e_g level could be placed in either the $d_{x^2-y^2}$ and d_{z^2} orbitals. Placing the odd electron in either orbital destroys the degeneracy of the e_g orbitals and usually has the effect of moving the ligands on one axis in or out. For Cu(II) complexes this effect is very common, resulting in longer bond lengths on what is usually taken as the complex's *z* axis. The effect is also seen for high-spin d^4 Mn(III) and for low-spin d^7 Co(II) and Ni(III) complexes.

TABLE 1.10 Splitting Values for d Orbitals in Common Geometries

C. N.[a]	Geometry	$d_{x^2-y^2}$	d_{z^2}	d_{xy}	d_{xz}	d_{yz}
4	Tetrahedral	–2.67	–2.67	1.78	1.78	1.78
4	Square planar[b]	12.28	–4.28	2.28	–5.14	–5.14
5	Square pyramidal[c]	9.14	0.86	–0.86	–4.57	–4.57
6	Octahedral	6.00	6.00	–4.00	–4.00	–4.00

[a] C. N. stands for coordination number.
[b] Bonds in xy plane.
[c] Pyramidal base in *xy* plane.

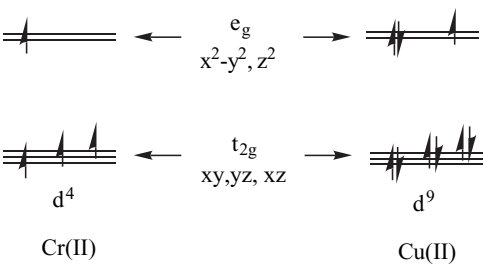

Figure 1.8 Electron configurations for high-spin Cr(II) and Cu(II).

1.7 BIOORGANOMETALLIC CHEMISTRY

Organometallic complexes obey the so-called eighteen-electron (18-e) and sixteen-electron (16-e) rules as described below. These rules may also be applied to bioinorganic (bioorganometallic) systems. According to 16- or 18-e rules, the valence electrons of transition metals are considered to be filling the 4*s*, 3*d*, 4*p* or 5*s*, 4*d*, 5*p* shells. The most stabilized filled shell is determined to be eighteen electrons—s^2, d^{10}, p^6, differing by the ten electrons of the filled *d* shell from main group element compounds stabilized by electron octets. Compounds or complexes fulfill the 18-e rule by addition of metal valence electrons and electron contributions from ligands. Metal valence shell electrons may be counted as if the metal, in its 0, +1, +2 oxidation states, combine with ligand electrons counted according to Table 1.11, which lists common ligands and their electron contributions. Table 1.11 counts electrons as if the ligands are neutral or are contributing electrons to the metal covalently. Another electron counting system classifies ligands according to an ionic contribution. Both these systems are more completely described in a website found at http://www.ilpi.com/organomet/electroncount.html.

Many stable coordination complexes can be counted as having sixteen electrons (16-e rule), especially those having square-planar geometry and those bonded to aromatic rings through their π electronic systems. Some of these complexes, belonging to a group of compounds called metallocenes, bind to DNA and have antitumor properties. Examples discussed in the literature usually contain two cyclopentadienyl ligands, η^5-cp, two chloride, Cl^-, ligands and the metals titanium, Ti, vanadium, V, molybdenum, Mo, or niobium, Nb. The complexes have the overall formula Cp_2MCl_2 and are named, for example, as titanocene, vanadocene, or molybdocene complexes. The titanium antitumor complex, *bis*-η^5-cyclopentadienyldichlorotitanium(II), Cp_2TiCl_2, is shown in Figure 1.9. This complex is the first metallocene, and the first non-platinum metal complex, to have undergone clinical trials as an anticancer agent.

TABLE 1.11 Ligand Contributions to the 16- or 18-Electron Rule

Ligand	Number of Electrons
Hydrogen $H^\bullet$, chloride radical $Cl^\bullet$	1
Alkyl (CH_3, CH_3CH_2, etc) or acyl (RC=O) groups	1
NO (bent)	1
Carbonyl groups ($RCOO^-$), CO, CN^-, RCN or RNC, ethers (ROR), sulfides (R_2S), ketones (R(C=O)R)	2
Lewis bases Cl^-, O^{2-}, S^{2-}, ammonia (NH_3), amines (NR_3), phosphines (PR_3)	2
Alkenes ($RCH=CH_2$)	2 per double bond
Nitrosyl group (NO) linear	3
Cyclopentadienyl, cp (C_2H_5)	5 per ring
Benzene (C_6H_6)	6 per ring (π donation)

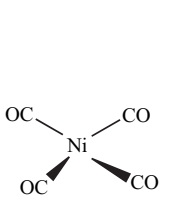

tetracarbonylnickel(0)
Ni(0) = 10 e ($4s^2 3d^8$)
4 CO = 8 e
Total = 18 e

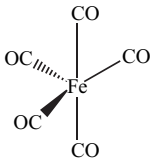

pentacarbonyliron(0)
Fe(0) = 8 e ($4s^2 3d^6$)
5 CO = 10 e
Total = 18 e

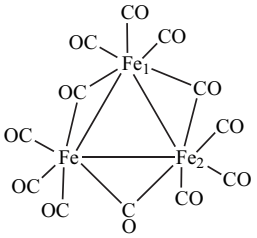

$Fe_1(0)$ = 8 e
3 terminal CO = 6 e
2 bridging CO = 2 e
2 Fe-Fe bonds = 2 e
Total = 18 e for each Fe

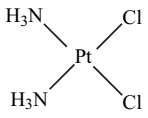

cis-dichlorodiammine-platinum(II)
Pt(II) = 8 e
2 NH_3 = 4 e
2 Cl^- = 4 e
Total = 16 e

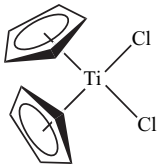

bis-η^5-cyclopentadienyl-dichlorotitanium(II)
Ti(II) = 2 e
2 cp = 10 e
2 Cl^- = 4 e
Total = 16 e

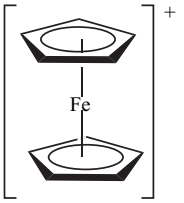

ferrocenium ion
Fe(I) = 7 e
2 cp = 10 e
+ charge = -1 e
Total = 16 e

Figure 1.9 Molecules obeying the 16-e and 18-e rules.

Structure–activity relationship studies have shown that the complex forms stable adducts with DNA.[11] Two unsubstituted cyclopentadienyl ligands appear to be important for activity because the compound $(MeCp)_2TiCl_2$ has been found to be biologically inactive. The corresponding molybdenum-containing metallocene, Cp_2MoCl_2, appears to have a different mode of cytotoxic (antitumor) activity because it does not form stable DNA adducts under the same conditions as the titanocene. Although the molybdocene readily forms soluble adducts with the amino acid cysteine and physiologically prevalent sulfur-containing compounds such as glutathione (see Figure 7.37), thiol derivatives of a molybdocene dichloride have been shown to lack antitumor activity. Researchers in the field have concluded that the biological chemistry of each of the metallocene dihalides is unique. The ongoing study of organometallic metallocenes as antitumor agents have been reported in various articles as referenced here.[12] The anticancer agent cisplatin, *cis*-dichlorodiammineplatinum(II), also obeys the 16-e rule.

Many organometallic complexes are clusters involving multiple metals that feature metal–metal bonds. The electrons in Me–Me bonds are counted by contributing one electron to each metal connected. Bridging ligands contribute one-half of their electrons to each metal center. Some simple examples in Figure 1.9 illustrate application of the rules.

Iron–sulfur clusters, such as those found in the enzyme aconitase discussed in Section 7.9.2.1, cannot be treated using the 16-e or 18-e rules. Other frameworks exist to treat large metal clusters, and these have some utility in treating $[Fe_xS_y]^{n+}$ clusters. One method treats the number of metal atoms and the metal-metal bonds in a cluster according to the following formula[13]:

$$\sum \text{Valence electrons} = \#\text{ of cluster Me atoms} \times 18 - (\text{no. of metal–metal bonds}) \times 2$$

Applying this formula to the cubane $[Fe(II)_4(\eta^5\text{-}C_5H_5)((\mu_3\text{-}S)_4]$ shown in Figure 1.10A results in the following electron count:

$$\sum \text{Valence electrons} = 4 \times 18 - (6 \times 2) = 60 \text{ electrons}$$

the so-called "magic number" for four metal atoms in a cluster.

If one applies the same procedure to Figure 1.10B, an iron–sulfur cluster often used as a model for those in biological systems, the same magic number of 60 would be obtained. Cluster magic numbers would occur as: 48 e for a triangular clusters, 60 e for tetrahedral, 72 e for trigonal bipyramidal, 74 e for square pyramidal, 84 e for octahedral complexes like $Zr_6I_{14}C$ or $[Mo_6Cl_{14}]^{2-}$ or 86 e for octahedral complexes such as $Rh_6(CO)_{16}$ and $[Os_6(CO)_{18}]^{2-}$, 90 e for trigonal prisms, and 120 e for cubic structures. Reference 13a contains a more complete discussion of cluster valence electron counting.

For biological systems such as ferredoxins, problems arise when counting electrons by the valence electron method. This system assumes six Fe–Fe bonds within the tetrahedral iron–sulfur clusters, but Fe–Fe bond distances within biological iron–sulfur clusters, as found by X-ray crystallography, often

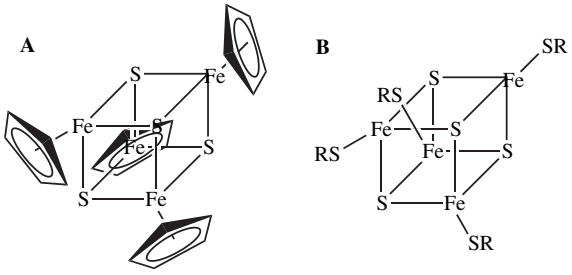

$[(Fe(II))_4(\eta^5\text{-}C_5H_5)_4(\mu_3\text{-}S)_4]$ $[(Fe(II))_4(SR)_4(\mu_3\text{-}S)_4]^{4-}$

Figure 1.10 Cubanes (A) $[Fe(II)_4(\eta^5\text{-}C_5H_5)_4(\mu_3\text{-}S)_4]$ and (B) $[Fe(II)_4(SR)_4(\mu_3\text{-}S)_4]^{4-}$.

do not indicate Fe–Fe bonds. It is known that for the Fe_4S_4 cubane found in biological systems, oxidations are accompanied by increasing distortion of the cubane frame. Nevertheless, ^{57}Fe Mössbauer spectra indicate that the four iron atoms remain equivalent, suggesting delocalization within the Fe–S framework. Most biological iron–sulfur clusters deviate substantially from the electron-counting rules for iron–sulfur clusters discussed here.

In this text, iron–sulfur clusters are discussed because they appear in proteins and enzymes: (1) cytochrome b(6)f, Rieske [2Fe–2S] cluster (Section 7.5 and Figure 7.26); (2) cytochrome bc_1, Rieske [2Fe–2S] cluster (Section 7.6 and Figure 7.30); and (3) aconitase, [4Fe–4S] cluster (Section 7.9.2.1, and Figure 7.50). The iron–sulfur protein (ISP) component of the cytochrome b(6)f and cytochrome bc_1 complexes, now called the "Rieske" ISP, was first discovered and isolated by John S. Rieske and co-workers in 1964 (in the cytochrome bc_1 complex). More information about the RISP is found in Section 7.5.1. Section 7.9.2 briefly discusses other proteins with iron–sulfur clusters—rubredoxins, ferrodoxins, and the enzyme nitrogenase. The nitrogenase enzyme was the subject of Chapter 6 in the first edition of this text—see especially the first edition's Section 6.3 for a discussion of iron–sulfur clusters. In this second edition, information on iron–sulfur clusters in nitrogenase is found in Section 3.6.4. See Table 3.2 and the descriptive examples discussed in Section 3.6.4.

Many systems in organometallic chemistry involve the activation of hard-to-oxidize alkanes or other organic moieties. In this regard, several metalloenzymes discussed in this text are efficient alkane oxidizers. Cytochrome P450 (Section 7.4) enzymes are monooxygenases that insert one atom of a dioxygen molecule into a wide variety of organic substrates. The other oxygen atom of the dioxygen molecule is converted to water during the P450 catalytic cycle. Methane monooxygenase (Section 7.9.3.1) catalyzes the conversion of the hardest-of-all-to-oxidize alkanes, methane, CH_4, to CH_3OH. Biomimetic bioinorganic researchers model the active centers of these metalloenzymes as small molecules, to learn more about the metalloenzyme's catalytic cycle, or to design efficient organometallic catalysts for industrial processes.

Researchers studying the metalloenzyme hydrogenase would like to design small compounds that mimic this enzyme's ability to reversibly reduce protons to H_2 and H_2 to $2H^+$, using an active center that contains iron and nickel. Cobalamins (vitamin B_{12} and its derivatives) contain an easily activated Co–C bond that has a number of biological functions, one of which is as a methyl transferase, 5-methyltetrahydrofolate-homocysteine methyltransferase (MTR). This enzyme converts homocysteine (an amino acid that has one more CH_2 group in its alkyl side chain than cysteine; see Figure 2.2) to methionine as methylcobalamin is converted to cobalamin.

1.8 ELECTRON TRANSFER

Many reactions catalyzed by metalloenzymes involve electron transfer. On the simplest level, one can consider electron transfer reactions to be complemen-

tary when there are equal numbers of oxidants and reductants and the metals transfer equal numbers of electrons as shown in equation 1.27:

$$Fe(III)(CN)_6^{3-} + Ru(II)(NH_3)_6^{2+} \rightarrow Fe(II)(CN)_6^{4-} + Ru(III)(NH_3)_6^{3+} \quad (1.27)$$

Noncomplementary reactions, as shown in equation 1.28, involve unequal numbers of oxidants and reductants because the number of electrons gained or lost by each metal differs.[6] Noncomplementary reactions, especially for large biomolecules, must proceed through a number of bimolecular steps since the possibility of termolecular or higher-order collisions is very small.

$$Mn^{7+} + 5Fe^{2+} \rightarrow Mn^{2+} + 5Fe^{3+} \quad (1.28)$$

Two types of electron transfer mechanisms are defined for transition metal species. Outer-sphere electron transfer occurs when the outer, or solvent, coordination sphere of the metal centers is involved in transferring electrons. No reorganization of the inner coordination sphere of either reactant takes place during electron transfer. A reaction example is depicted in equation 1.29:

$$Fe(II)(CN)_6^{4-} + Rh(IV)Cl_6^{2-} \rightarrow Fe(III)(CN)_6^{3-} + Rh(III)Cl_6^{3-} \quad (1.29)$$

Inner-sphere electron transfers involve the inner coordination sphere of the metal complexes and usually take place through a bridging ligand. The classic example, typical of those studied and explained by H. Taube,[14] is illustrated by Figure 1.11's reaction sequence adapted from reference 7. In this reaction sequence, production of $[Cr(III)(H_2O)_5Cl]^{2+}$ implies that electron transfer through the bridged intermediate from Cr(II) to Co(III) and Cl^- transfer from Co to Cr are mutually interdependent acts.

Harry B. Gray and Walther Ellis, writing in Chapter 6 of reference 15, describe three types of oxidation–reduction centers found in biological systems. The first of these, protein side chains, may undergo oxidation–reduction reactions such as the transformation of two cysteine residues to form the cystine dimer as shown in equation 1.30:

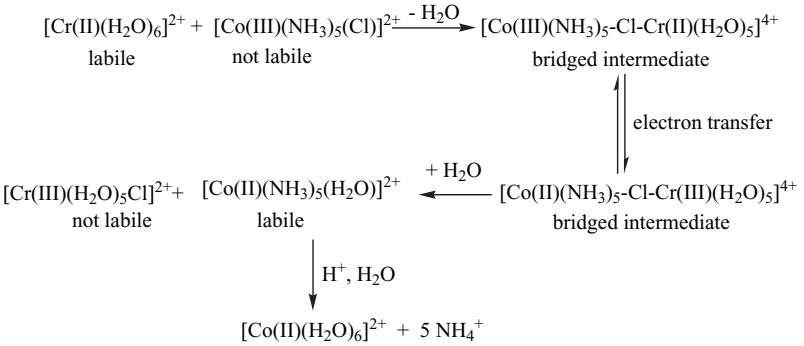

Figure 1.11 An inner-sphere electron transfer reaction sequence. (Adapted from reference 7, p. 208. Copyright 1995, Wiley-VCH.)

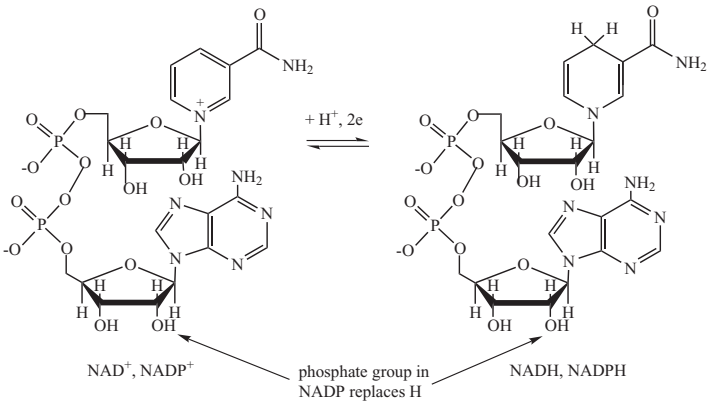

Figure 1.12 Electron transfer cofactors NAD^+ or $NADP^+$.

$$2R{-}SH \rightarrow R{-}S{-}S{-}R \tag{1.30}$$

The second type of biological electron transfer involves a variety of small molecules both organic and inorganic. Examples of these are nicotinamide adenine dinucleotide (NAD) and nicotinamide adenine dinucleotide phosphate (NADP) as two electron carriers and quinones and flavin mononucleotide (FMN) that may transfer one or two electrons. The structure of NAD and its reduced counterpart NADH are shown in Figure 1.12.

The third type of biological electron transfer involves metalloproteins themselves. These may be electron carriers (i.e., cytochromes) or proteins involved in the transport or activation of small molecules (i.e., cytochrome c oxidase). These so-called electron transferases have some or all of the following characteristics: (1) a suitable cofactor, such as NAD^+/NADH or another protein, acting as an electron source or sink; (2) geometry that allows the cofactor close enough to the protein surface for the transfer of electrons; (3) a hydrophobic shell on the protein surface around or near the cofactor; and (4) architecture permitting changes in protein conformation to facilitate electron transfer. These last changes should be small.[16] Electron transferases that will be discussed in this text include the cytochromes and cytochrome c oxidase (Chapter 7). Cytochromes comprise several large classes of electron transfer metalloproteins widespread in nature. At least four cytochromes are involved in the mitrochondrial electron transfer chain that reduces oxygen to water according to equation 1.31.

Other electron transferases include the rubredoxin and ferredoxin iron–sulfur proteins, so named because they contain iron–sulfur clusters of various sizes. Rubredoxins are found in anaerobic bacteria and contain iron ligated to four cysteine sulfurs. Ferredoxins are found in plant chloroplasts and mammalian tissue and contain spin-coupled [2Fe–2S] clusters. Further discussion of rubredoxin and ferredoxin proteins can be found in Chapters 6 and 7 of reference 15, and cytochromes will be extensively discussed in Chapter 7 of this text.

$$\frac{1}{2}O_2 + NADH + H^+ \rightarrow H_2O + NAD^+ \quad (1.31)$$

The simplest electron transfer reactions are outer sphere. The Franck–Condon principle states that during an electronic transition, electronic motion is so rapid that the metal nuclei, the metal ligands, and solvent molecules do not have time to move. In a self-exchange example,

$$A_{ox^*} + A_{red} \rightarrow A_{red^*} + A_{ox} \quad (1.32)$$

the energies of donor and acceptor orbitals as well as bond lengths and bond angles remain the same during efficient electron transfer. Figure 1.13A illustrates this behavior using Marcus theory potential energy diagrams. In a cross reaction between two different species (as illustrated in Figure 1.13B), one can write the following set of equilibrium statements (K) and rate equations (k_{et}):

$$A_{ox} + B_{red} \Leftrightarrow [A_{ox}B_{red}]\,(\text{precursor complex}) \quad (1.33)$$

$$[A_{ox}B_{red}] \xrightarrow{k_{et}} [A_{red}B_{ox}]\,(\text{successor complex}) \quad (1.34)$$

$$[A_{red}B_{ox}] \xrightarrow{\text{fast}} A_{red} + B_{ox} \quad (1.35)$$

Electron transfer theory is further explained in a classic paper published by Rudolph A. Marcus using potential energy diagrams to describe electron transfer processes.[17] In the diagrams such as shown in Figure 1.13, electron donors and acceptors behave as collections of harmonic oscillators. The diagram expresses donor and acceptor in a single surface representing the precursor complex and one representing the successor complex. Point S represents the activated complex and E_R and E_P are the reactant and product surfaces, respectively.

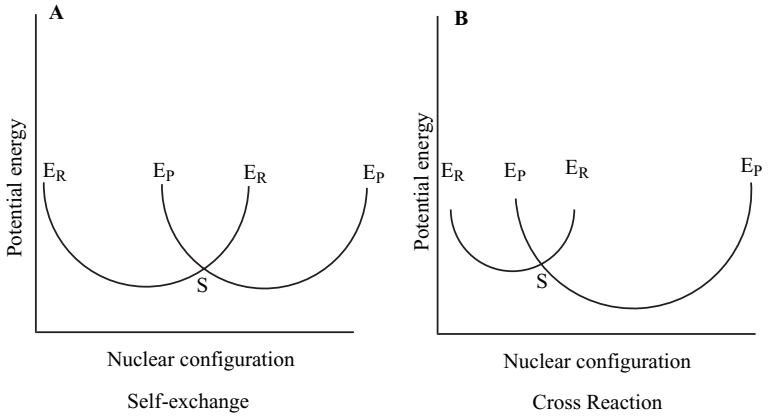

Figure 1.13 Potential energy diagrams describing electron transfer processes according to Marcus theory. (A) Self-exchange, (B) cross reaction.

It is beyond the scope of this text to continue the discussion of Marcus theory. Qualitatively the student should understand that electrons must find a path through the protein from the donor species to the acceptor. This may take place through bonds as outlined above or through electron tunneling events in which electrons travel through space between orbitals of the donor species to the acceptor species. Chapter 6 of reference 15 presents a clear explanation for further reading.

A four-day symposium held at the September 2006 meeting of the American Chemical Society honored Marcus' work on electron-transfer and reaction-rate theories and included talks by researchers continuing to use and update these theories in biological contexts. Recent biological system electron transfer experiments include oxygen binding and transport, photosynthesis, cellular respiration, and long-range electron transfer in proteins and DNA. One example comes from the laboratory of Alexei A. Stuchebrukhov, where a computational model is being developed to describe the proton-pumping mechanism of cytochrome c oxidase (to be discussed here in Section 7.8).[18] Essentially, the membrane-bound protein cytochrome c oxidase in mitochondria catalyzes the four electron reduction of O_2 to water using electrons and protons. The free energy generated by the reduction is used to "pump" protons to the outside of the mitochondrial membrane, generating an electrochemical gradient. The energy stored by this gradient is then used to synthesize adenosine triphosphate (ATP), the key energy transfer molecule involved in converting food into energy. The coupling of electron and proton transfer in cytochrome c oxidase is not well understood and is a subject of ongoing research in many bioinorganic laboratories.

An example of the need for extension of Marcus electron transfer theory was provided by Jacqueline K. Barton, one of Marcus' colleagues at the California Institute of Technology. Barton's group studies charge transport in DNA, attempting to elucidate fundamental mechanisms and kinetics of electron transport through DNA. A second research arm in the same laboratory studies how DNA becomes damaged in the genome and how this damage may be sensed and repaired. Experimental evidence indicates that DNA base excision repair proteins may use DNA charge transport to localize repair enzymes near the damage site. In both research areas, Barton describes the need for more theory to explain experimental results, particularly where ground-state DNA charge transport is monitored electrochemically.[19] Other biological applications of Marcus electron transfer and reaction rate theories described at the 2006 ACS symposium can be found in the *C&E News* article referenced here.[20]

1.9 CONCLUSIONS

The preceding brief review of inorganic chemistry has been oriented toward questions that will arise in subsequent discussion of bioinorganic systems. The

inorganic and bioinorganic chemistry texts referenced earlier in this chapter and here are good sources for answering the additional questions sure to arise in studying the behavior of metals in biological systems.[21] It is important to keep in mind that metal behavior in the biological milieu will be influenced greatly by the surroundings. Metal–ligand systems existing in thermodynamic equilibrium and slow to react to changing cellular or noncellular dynamics will not long endure. Therefore, most of the metalloenzyme systems to be described in following chapters contain metals in distorted and changeable ligand fields. These systems will continue to challenge the ingenuity of inorganic and bioinorganic chemists attempting to understand, modify, model, or design synthetic substitutes for them.

REFERENCES

1. Schwarz, K. *Ged. Proc.*, 1974, **33**, 1748–1757.
2. Frieden, E. *J. Chem. Ed.*, 1985, **62**(11), 917–923.
3. Frausto Da Silva, J. R. R.; Williams, R. J. P. *The Biological Chemistry of the Elements: The Inorganic Chemistry of Life*, Clarendon Press, New York, 1991.
4. Lippard, S. J.; Berg, J. M. *Principles of Bioinorganic Chemistry*, University Science Books, Mill Valley, CA, 1994.
5. Hay, R. W. *Bio-Inorganic Chemistry*, Ellis Horwood Limited, Halsted Press, New York, 1984.
6. Cowan, J. A. *Inorganic Biochemistry, An Introduction*, 2nd ed., Wiley-VCH, New York, 1997.
7. Cotton, F. A.; Wilkinson, G.; Gaus, P. L. *Basic Inorganic Chemistry*, 3rd ed., John Wiley & Sons, New York, 1995, pp. 192–194.
8. (a) Eigen, M. *Pure Appl. Chem.* 1963, **6**, 105. (b) Bennetto, H. P.; Caldin, E. F. *J. Chem. Soc. A*, 1971, 2198.
9. Tobe, M. L. Substitution Reactions, in *Comprehensive Coordination Chemistry*, Wilkinson, G., ed., Pergamon Press, Oxford, 1987, pp. 281–329.
10. Shriver, D. F.; Atkins, P. W.; Langford, C. H. *Inorganic Chemistry*, Oxford University Press, Oxford, 1990, pp. 477–478.
11. Waern, J. B.; Harding, M. M. *Inorg. Chem.*, 2004, **43**(1), 206–213.
12. (a) Waern, J. B.; Harris, H. H.; Lai, B.; Cai, Z.; Harding, M. M.; Dillon, C. T. *J. Biol. Inorg. Chem.*, 2005, **10**(5), 443–452. (b) Waern, J. B.; Dillon, C. T.; Harding, M. M. *J. Med. Chem.*, 2005, **48**(6), 2093–2099. (c) Caruso, F.; Rossi, M. *Met. Ions Biol. Syst.*, 2004, **42**, 353–384.
13. (a) Wheeler, R. A.; Hoffmann, R. *J. Am. Chem. Soc.*, 1986, **108**, 6605–6610. (b) Mingos, D. M. P. *Acc. Chem. Res.*, 1984, **17**, 311–319. (b) Mingos, D. M. P., in *Comprehensive Organometallic Chemistry*, Wilkinson, G.; Stone, F. G. A.; Abel, E. W., eds., Pergamon, Oxford, 1981. (c) Elschenbroich, C. *Organometallics: A Concise Introduction*, VCH, New York, 1992.
14. Taube, H. *Electron Transfer Reactions of Complex Ions in Solution*, Academic Press, New York, 1970.

15. Gray, H. B.; Ellis, W. R., in Bertini, I.; Gray, H. B.; Lippard, S. J.; Valentine, J. S. *Bioinorganic Chemistry* University Science Books, Mill Valley, CA, 1994, pp. 315–363.
16. Adman, E. T. *Biochim. Biophys. Acta*, 1979, **549**, 107–144.
17. Marcus, R. A. *Annual Rev. Phys. Chem.*, 1964, **15**, 155–196.
18. (a) Quenneville, J.; Popovic, D. M.; Stuchebrukhov, A. A. *Biochim. Biophys. Acta*, 2006, **1757**(8), 1035–1046. (b) Popovic, D. M.; Stuchebrukhov, A. A. *FEBS Lett.*, 2004, **566**(1–3), 126–130. (c) Popovic, D. M.; Stuchebrukhov, A. A. *J. Am. Chem. Soc.*, 2004, **126**(6), 1858–1871.
19. (a) Yavin, E.; Stemp, E. D.; O'Shea, V. L.; David, S. S.; Barton, J. K. *Proc. Natl. Acad. Sci. USA*, 2006, **103**(10), 3610–3614. (b) Shao, F.; Augustyn, K.; Barton, J. K. *J. Am. Chem. Soc.* 2005, **127**(49), 17445–17452. (c) Yavin, E.; Boal, A. K.; Stemp, E. D.; Boon, E. M.; Livingston, A. L.; O'Shea, V. L.; David, S. S.; Barton, J. K. *Proc. Natl. Acad. Sci. USA*, 2005, **102**(10), 3546–3551. (d) Williams, T. T.; Dohno, C.; Stemp, E. D.; Barton, J. K. *J. Am. Chem. Soc.*, 2004, **126**(26), 8148–8158.
20. Ritter, S. K. *C&E News*, 2006, **84**(42), 45–48.
21. (a) Cotton, F. A.; Wilkinson, G.; Murillo, C. A.; Bochmann, M. *Advanced Inorganic Chemistry*, 6th ed., John Wiley & Sons, New York, 2006. (b) Atkins, P.; Overton, T.; Rourke, J.; Weller, M.; Armstrong, F. *Inorganic Chemistry*, 4th ed., Oxford University Press, Oxford, 2006. (c) Shriver, D.; Atkins, P. *Inorganic Chemistry*, 4th ed., W. H. Freeman, New York, 2006. (d) Fraústo da Silva, J. R. R. *The Biological Chemistry of the Elements*, Oxford University Press, Oxford, 2001. (e) Kraatz, H.-B.; Metzler-Nolte, N., eds. *Concepts and Models in Bioinorganic Chemistry*, John Wiley & Sons, New York, 2006. (f) *Biological Inorganic Chemistry: Structure and Reactivity*, University Science Books, New York, 2007.